Earth Systems and Environment (2020) 4:535–550
https://doi.org/10.1007/s41748-020-00181-7

ORIGINAL ARTICLE

Comparison of MODIS- and CALIPSO-Derived Temporal Aerosol Optical Depth over Yellow River Basin (China) from 2007 to 2015

Ziyue Zhang[1] · Miao Zhang[1] · Muhammad Bilal[2] · Bo Su[1] · Chun Zhang[1] · Liuna Guo[1]

Received: 19 August 2020 / Accepted: 8 September 2020 / Published online: 26 September 2020

Abstract

In this study, Collection 6.1 (C6.1) of different aerosol optical depth (AOD) products of different spatial resolutions were used from the aqua moderate resolution imaging spectroradiometer (MODIS) including dark target (DT), deep blue (DB), deep blue (DB), and DT-DB (DTB). These products were compared with cloud-aerosol lidar, and infrared pathfinder satellite observation (CALIPSO) AOD retrievals over the Yellow River Basin (YERB), China from 2003 to 2017. The YERB was divided into three sub-regions, namely $YERB_1$ (the mountainous terrain in the upper reaches of the YERB), $YERB_2$ (the Loess Plateau region in the middle reaches of the YERB), and $YERB_3$ (the plain region downstream of the YERB). Errors and agreement between MODIS and CALIPSO data were reported using Pearson's correlation (R) and relative mean bias (RMB). Results showed that the CALIPSO whole layers AOD (AOD_S) were better matched with MODIS AOD than the CALIPSO lowest layer AOD (AOD_1). The time series of AOD shows higher values in spring and summer, and a small difference in AOD products was observed in autumn. The overall average value of CALIPSO AOD and MODIS AOD both fitted the order: $YERB_3 > YERB_2 > YERB_1$. The CALIPSO AOD retrievals have the best consistency with the DTB10K and the lowest consistency with DT3K. Overall, the regional distributions of the CALIPSO AOD and MODIS AOD are significantly different over the YERB, and the difference is closely related to the season, region, and topography. This study can help researchers understand the difference of aerosol temporal and spatial distribution utilizing different satellite products over YERB, and also can provide data and technical support for the government in atmospheric environmental governance over YERB.

Keywords MODIS · CALIPSO · AOD · Yellow river basin

1 Introduction

Atmospheric aerosols are solid and liquid particles with a size between 0.01 and 100 nm, which have complex physical, chemical, and optical characteristics (Nichol et al. 2020; Tian et al. 2018). Aerosols have a considerable impact on climate, atmospheric environment quality, human health, and related matters (Ali et al. 2020; Kaiser and Granmar 2005; Kaufman et al. 2002; Kulmala et al. 2013; Lelieveld et al. 2015; Sun and Ariya 2006). Aerosols can scatter or absorb solar radiation, causing changes in the earth–air radiation budget and affecting the radiation balance of the earth system (Butt et al. 2016; Dubovik et al. 2012). At the same time, due to the irregular spatial and temporal distribution of aerosols, which varies greatly with time, their optical and physical characteristics are unstable. Therefore, long-term observation of aerosols is a key requirement for studying the characteristics of aerosols (Bilal et al. 2014; Han et al. 2018; Miao et al. 2020; Misra et al. 2008). Aerosols are also responsible for environmental pollution; they are major components of haze, dust, and other extreme weather conditions. The study of aerosols can also deepen researchers' understanding of their environmental effects and provide

Ziyue Zhang and Miao Zhang equally contributed to this study.

✉ Miao Zhang
zm_liesmars@nynu.edu.cn

✉ Muhammad Bilal
muhammad.bilal@connect.polyu.hk

[1] School of Environmental Science and Tourism, Nanyang Normal University, Wolong Road No.1638, Nanyang 473061, China

[2] School of Marine Sciences, Nanjing University of Information Science and Technology, Nanjing 2100444, China

theoretical support for decision-makers to introduce corresponding environmental protection policies (Development 2014; Edenhofer and Seyboth 2013; Gong et al. 2015; Magistrale 1992; Tie et al. 2009; Zhang et al. 2014a).

Aerosol optical depth (AOD) is the most basic optical characteristic parameter of atmospheric aerosols and is the key factor in characterizing atmospheric turbidity and determining the climatic effect of aerosols(Zhang et al. 2014b). AOD is often used in studies of how aerosols affect regional climates and the temporal and spatial variation characteristics of the atmosphere (Jing et al. 2018; Kang et al. 2016; Rosenfeld 2000; Wang et al. 2019). At present, research on AOD depends mainly on satellite-based remote sensing and ground-based remote sensing dataset. The National Aeronautics and Space Administration (NASA) has established the ground-based aerosol robotic network (AERONET) around the world. Also, China has established the ground-based China aerosol remote sensing network (CARSNET) in the country to conduct a long-term observation of the aerosol's variation features. The results obtained from both these ground-based stations showed good findings (Che et al. 2014; Kleidman et al. 2005; Qin et al. 2018; Shi et al. 2019). The aerosol data observed by ground-based remote sensing are highly accurate, but the distribution of sites is very sparse, and the spatial distribution of aerosols features over large areas and at large scale cannot be obtained (Che et al. 2015; Ming et al. 2017). Satellite passive remote sensing can obtain AOD retrievals over large areas, as is done by the moderate resolution imaging spectroradiometer (MODIS) of onboard on Terra and Aqua satellites, which can make up for the deficiency that the ground observation data cannot represent the spatial distribution and the overall trend of aerosol changes. Besides, the active lidar remote sensing satellite CALIPSO (cloud-aerosol lidar and infrared pathfinder satellite observation), is equipped with cloud-aerosol lidar with orthogonal polarization (CALIOP), which provides not only large-scale, planar aerosol optical properties products but also three-dimensional spatial and temporal information of the aerosol vertical distribution (Marchant et al. 2020; Winker et al. 2007, 2003, 2009). This provides a powerful tool for the more comprehensive acquisition of aerosol optical and physical characteristics (Kato et al. 2012; Yu et al. 2015).

MODIS AOD products have the advantages of high retrieval accuracy, long time series, and good spatial coverage, which have been validated by a large number of international scholars to have significant application value in aerosol research (Ali and Assiri 2019; Ali et al. 2019; Tian et al. 2018). Since MODIS aerosol products are updated frequently, many scholars have carried out a large number of verification studies of new MODIS AOD products by comparing them with AERONET or CARSNET ground-based remote sensing data (Bilal et al. 2018; Che et al. 2015; Dubovik et al. 2012; He et al. 2017; Shi et al. 2019; Wang et al. 2019). Zhang et al. (2019b) evaluated the performance of MODIS Collection C6.1 (C6.1) AOD products over the Yellow River basin (YERB) by comparing the AOD data from ground-based CARSNET site and obtained good results (Zhang et al. 2019b). The study suggested that no single satellite AOD product performed satisfactorily over YERB. On the other hand, the verification of CALIPSO satellite products has been carried out less frequently by previous studies (Zhang et al. 2019a). The main reason might be that the location of the substellar point of CALIPSO is difficult to match precisely with the few ground-based sites, making it difficult to verify the CALIPSO aerosol products. Therefore, we decided to compare the MODIS and CALISPO products with each other to indirectly verify the performance of CALIPSO, based on the previous research results of MODIS-CARSNET obtained from the studies of Zhang et al. (2019a) and Zhang et al. (2019b). On the other hand, the performance of CALIPSO was good in studying the properties of the lowest aerosol layers over YERB. So it is important to the MODIS- and CALIPSO-derived AOD over YERB (Kumar et al. 2018; Shi et al. 2020; Yang et al. 2020).

In recent years, as the environmental issues faced by China have grown to an unprecedented scale, researchers have placed much emphasis on studying the optical, physical, and distribution characteristics of aerosols in the Yangtze River delta, Beijing–Tianjin–Hebei, the Pearl River delta, and other important developed areas (Bilal et al. 2019, 2013, 2014; Deng et al. 2008; Jie et al. 2017; Liu et al. 2008; Shen et al. 2015; Xia et al. 2016). Those authors obtained the long-term temporal variation and spatial distribution of the aerosols, but less research has been carried out with regard to the aerosol distribution characteristics over YERB (Zhang et al. 2019b). The YERB is located in the north-central part of mainland China and lies in an east–west direction across the country. The sub-regions of the YERB have obvious differences in topographical distribution. The regional economies and industrial development of the YERB sub-regions have even more imbalance. Long-term accurate monitoring of aerosol optical physical characteristics and their spatiotemporal distributions over each sub-region of the YERB has important practical significance for the protection of the atmospheric environment over the YERB (Zhang et al. 2019b). According to the characteristics of the YERB, this paper evaluates the performance of the CALIPSO AOD product over the YERB by comparing it with the Aqua MODIS C6.1 AOD products. The study is organized as follows: the study area is described in Sect. 2, the data used and the methodology are described in Sect. 3, the results and discussion are presented in Sect. 4, and finally, the conclusions are summarized in Sect. 5.

2 Study Area

The YERB is located between 95° E and 120° E and between 30° N and 45° N (Fig. 1). Due to the large area of the YERB and to better study the characteristics of AOD in different sections of the YERB, this paper divides the YERB into three regions; the upper reaches of the Yellow River, with forest mountains and perennial snow on the mountain peaks ($YERB_1$: 30° N–38° N, 95° E–105° E); the middle reaches of the Yellow River, dominated by the loess plateau ($YERB_2$: 33° N–43° N, 105° E–112° E); and the lower reaches of the Yellow River, dominated by the plain ($YERB_3$: 31° N–39° N, 112° E–119° E). The Yellow River originates from the northern foot of Bayan Kara Mountain in the central part of Qinghai province and flows through nine provinces and regions, namely Qinghai, Gansu, Sichuan, Ningxia, Inner Mongolia, Shaanxi, Shanxi, Henan, and Shandong, with a total length of 5464 km. It is about 1900 km long from east to west and 1100 km wide from north to south, draining a watershed area of about 795,000 km^2 (Wang et al. 2007).

The YERB is a vast area with complex terrain, spanning four geomorphic units: the Qinghai–Tibet plateau, the Inner Mongolia Plateau, the Loess Plateau, and the North China plain. The height difference between east and west is significant (the maximum height difference is 4480 m), and the range of climates along the basin is quite dramatic. From a monsoon perspective, the area west of Lanzhou in the upper reaches of the Yellow River (YERB1) belongs to the Qinghai–Tibet plateau monsoon region, while the other areas are temperate and subtropical monsoon regions. The temperature is warmer in the southeast (YERB3) than in the northwest (YERB1) and is cooler over mountains than over plains in the YERB. The economy of the YERB is relatively undeveloped except for the estuaries, especially in the upper reaches of the Yellow River in the west (YERB1), which is an area of lower elevation (Wang et al. 2007; Yang et al. 2020). Therefore, the study of the AOD characteristics in the YERB is of great scientific significance to reveal the influence of aerosols on climate under different regional environmental conditions.

3 Data Used and Methodology

3.1 MODIS C6.1 Data

The Aqua-MODIS Level 2 C6.1 aerosol products were downloaded from the Level-1 and Atmosphere Archive and Distribution System Distributed Active Archive Center (LAADS DAAC) (https://ladsweb.modaps.eosdis.nasa.gov/). The inversion of the MODIS C6.1 AOD product is based mainly on the dark target (DT) algorithm and the deep

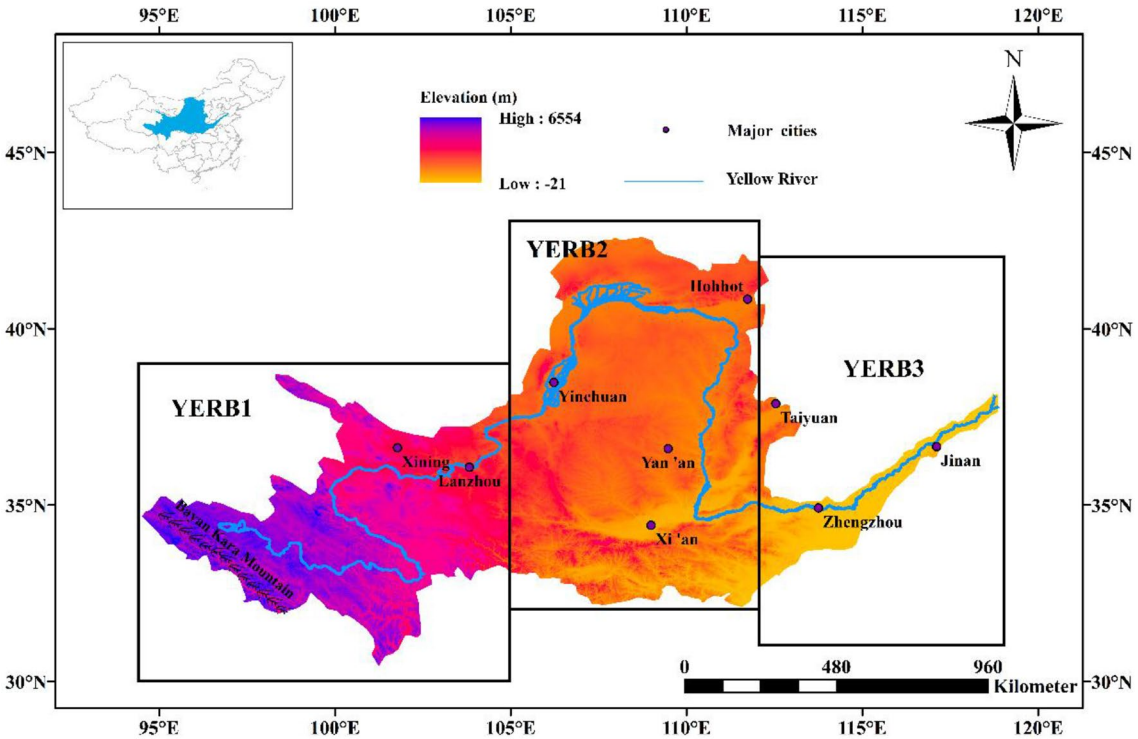

Fig. 1 Geographical locations of the Yellow River Basin (YERB). The color bar represents the elevation

blue (DB) algorithm. The DT algorithm was developed to provide AOD retrievals over dark surfaces, and currently, it provides AOD retrievals over land at 3 km or 10 km resolutions. The results show that, on a global scale, more than 70.6% of DT retrievals are within the estimated confidence envelope of one standard deviation, which is approximately $\pm(0.05+15\%)$ (Tian et al. 2018). The DB algorithm was developed to retrieve aerosol properties over the bright desert (Bilal et al. 2014; Gupta et al. 2016; Jie et al. 2017; Levy et al. 2013). The expected error (EE) of the DB algorithm for AOD over land is approximately $\pm(0.05+20\%)$, and 79% of retrievals agree within the EE of the corresponding AERONET observation (Hsu et al. 2013; Shi et al. 2019). In this paper, Aqua-MODIS C6.1 (MYD04) DT AOD retrievals at 3 km (DT3K) and 10 km (DT10K) resolutions, the DB AOD retrievals at 10 km (DB10K), and combined DT and DB AO retrievals at 10 km resolution (DTB10K) are obtained for comparison with CALIPSO data. Table 1 shows the scientific data set of the Aqua-MODIS C6.1 AOD products used in this study between January 1, 2003, and December 31, 2017. In this study, only the best quality flag (QA = 3) data were considered.

3.2 CALIPSO Data

CALIPSO is an earth-probing satellite project started jointly by NASA's Langley Research Center (LaRC) and the National Space Research Center of France in 2006. CALIPSO provides the three-dimensional distribution of clouds and aerosols at global scales every 16 days. CALIOP is one of the main instruments on the CALIPSO satellite. It has one 1064 nm wavelength channel and two 532 nm wavelength polarization channels. It can observe clouds and aerosols backscattering information between latitudes of 82° north and south (Huang et al. 2008; Winker et al. 2007, 2009; Yu et al. 2015). CALIOP can detect the vertical distribution of clouds and aerosols more accurately by utilizing the backscatter it receives at each level within the atmosphere. At the same time, CALIOP is an active remote sensing instrument that can operate during both day and night without interference from the earth's surface, and free from the excessive dependence of passive remote sensing on short-wave solar radiation (Liu et al. 2008; Omar et al. 2009; Winker et al. 2007). Therefore, the CALIPSO satellite provides a clean and comprehensive set of measurements for the study of the vertical structure and transmission of aerosols.

The CALIPSO lidar has six main levels of data: levels 4, 3, 2, 1B, 1A, and 0. Level 2 data products include three types, namely: vertical feature layer products, layer products, and profile data products (Winker et al. 2003). The aerosol layer products are generated based on the raw CALIPSO profile data (https://www-calipso.larc.nasa.gov/about/atrain.php) using the selective iterated boundary locator (SIBYL) algorithm (Winker et al. 2009; Yu et al. 2015). Using SIBYL, the feature layers are detected in every raw data profile, then the amount (number) of aerosol feature layers (N) and the heights of the feature layer's base (HB_N) and top (HT_N) are obtained. The data contain at most eight vertical layers ($N \le 8$) spanning the entire atmosphere in every raw data profile.

In this study, the AOD of the lowest aerosol layer (AOD_1, if $N=1$ in Eq. (1)) and the sum of the AOD from all the aerosol layers (AOD_S, Eq. (2)) were the main variables used for comparative analysis with the four MODIS products:

$$\mathrm{AOD}_N = \int_{\mathrm{HB}_N}^{\mathrm{HT}_N} \delta(z)\mathrm{d}z; \quad N = 1, 2, \ldots, 7, 8, \tag{1}$$

$$\mathrm{AOD}_\mathrm{S} = \sum_{1}^{N} \mathrm{AOD}_N; \quad N = 1, 2, \ldots, 7, 8. \tag{2}$$

3.3 Comparison Methods

Since both CALIPSO and Aqua are part of the "A-Train" constellation and the data are spaced just a few minutes apart, there is only a small observation time difference between them, which allows them to be used for a comparative study. In this paper, CALIPSO and Aqua daytime Level 2 aerosol layer products at 550 nm were mainly used, and the selected data overlap time range was from January 1, 2007, to December 31, 2014. In the study area, MODIS produces multiple images every day, but they do not completely cover the study area, so multiple images need to be combined. Moreover, the CALIPSO data are vertical linear data, so the two types of data cannot be directly compared. Meanwhile, since the spatial

Table 1 Scientific data set of the Aqua-MODIS C6.1 AOD products used in this study from January 1, 2003, to December 31, 2017

Satellite	Product	Aerosol optical depth
Aqua_MYD04	DT3K	Optical_Depth_Land_And_Ocean
	DT10K	Optical_Depth_Land_And_Ocean
	DB10K	Deep_Blue_Aerosol_Optical_Depth_550_Land
	DTB10K	AOD_550_Dark_Target_Deep_Blue_Combined

resolution of each pixel in the MODIS image is 3 km or 10 km and there is no spatial resolution information of the substellar point of CALIPSO, it is very complex to match and screen the location of the MODIS pixel and the substellar point of the CALIPSO orbit transit. To facilitate data matching on the same time series, the MODIS and CALIPSO data applied in the research area were interpolated and resampled onto a grid of $1^\circ \times 1^\circ$, and the data over the research area were clipped out using a vector mask file. The linear mean interpolation technique is used, and if the latitude and longitude are in one grid, the mean value is considered as the final value. Then the data of the study area were statistically analyzed and compared on a seasonal and yearly basis for each of the three sub-regions of the YERB.

To report accuracy and errors in the AOD retrievals, the following statistical parameters are used to evaluate the correlation of several values: the slope, *y*-intercept, Pearson's correlation (*R*), root mean square error (RMSE, Eq. (3)), expected error (EE, Eq. (4)), the relative mean bias (RMB, Eq. (5)), and mean absolute error (MAE, Eq. (6)).

$$\mathrm{RMSE} = \sqrt{\frac{1}{n}\sum_{i=1}^{n}\left(\mathrm{AOD}_{(\mathrm{MODIS})_i} - \mathrm{AOD}_{(\mathrm{CALIPSO})_i}\right)^2}, \quad (3)$$

$$\mathrm{EE} = \pm\left(0.05 + 0.15\mathrm{AOD}_{\mathrm{MODIS}}\right), \quad (4)$$

$$\mathrm{RMB} = \frac{\mathrm{AOD}_{(\mathrm{MODIS})_i}}{\mathrm{AOD}_{(\mathrm{CALIPSO})_i}}, \quad (5)$$

$$\mathrm{MAE} = \frac{1}{n}\sum_{i=1}^{n}\left|\mathrm{AOD}_{(\mathrm{MODIS})_i} - \mathrm{AOD}_{(\mathrm{CALIPSO})_i}\right|. \quad (6)$$

4 Results and Discussion

4.1 Comparison of Aqua-MODIS C6.1 AOD with CALIPSO AOD

Figure 2 shows scatter plots of the MYD04 C6.1 DT3K AOD against CALIPSO AOD for the period of January 1, 2007, to December 31, 2014, over the YERB in spring, summer, autumn, and winter. In Fig. 2, a total of 1427 observations of DT3K data are matched with the CALIPSO data. The results show poor correlation between DT3K and CALIPSO (AOD_1 and AOD_S); for example, R is only 0.35 and 0.40 for AOD_1 and AOD_S, respectively; RMSE was 0.35 for AOD_1 and 0.34 for AOD_S; 35.18% of retrievals were within the EE for AOD_1 and 52.07% for AOD_S; 7.71% and 12.89% of retrievals were below the EE, and 57.11% and 35.04% of retrievals were above, for AOD_1 and AOD_S, respectively. Moreover, the values of RMB (1.90 and 1.37) and MAE (0.18 and 0.10) were significantly higher. According to these results, the DT3K AOD values were significantly greater than those of CALIPSO, and the differences between DT3K and AOD_1 are significantly higher than the differences between DT3K and AOD_S. This is because AOD_1 only represents the AOD of the lowest aerosol, while AOD_S represents the sum of the AOD over all layers. The AOD product of MODIS considers

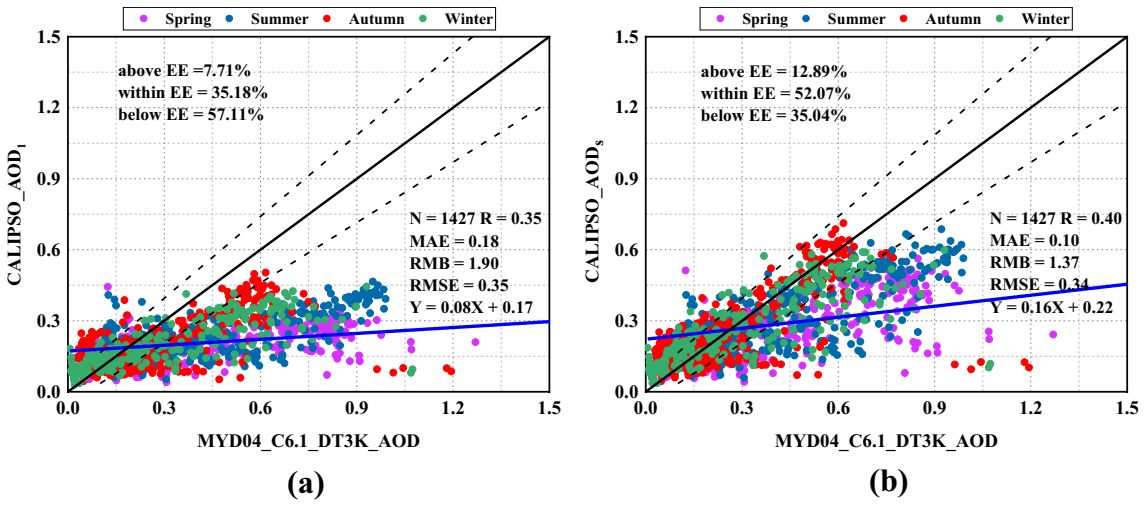

Fig. 2 Validation of the CALIPSO AOD_1 (**a**) and CALIPSO AODs (**b**) for the period of January 1, 2007 to December 31, 2014 against MYD04 C6.1 DT3K (**a**) AOD for the period of January 1, 2003 to December 31, 2017 over the YERB. The black solid line is the 1:1 line, the black dashed lines indicate the envelope of the EE, and the blue line is the regression line

the whole atmosphere, not just the lowest aerosols, so the matching between AOD_S and C6.1 DT3K is better.

Table 2 provides the statistical parameters of MYD04 C6.1 DT3K versus the CALIPSO AOD for the four seasons. The comparison shows that the degree of matching of MYD04 C6.1 DT3K-CALIPSO AOD_1 and MYD04 C6.1 DT3K-AOD_S in different seasons has a similar and large seasonal difference. Among these parameters, the value of the correlation coefficient R is within the range of 0.19–0.69 and 0.19–0.78 for AOD_1 and AOD_S, respectively. The proportion of matching data falling within the EE is 24.40–45.76% and 43.16–63.24% for AOD_1 and AOD_S, respectively. Furthermore, with the values of *R* being largest in summer (0.78) and the values within EE (63.24%) being largest in autumn, this numerical behavior indicates that, despite the good correlation coefficient, the C6.1 DT3K products still could not meet the EE standard. Almost 41.39–70.78% and 15.68–50.94% of the collocations fell below the EE for AOD_S and AOD_1, respectively; at the same time, except for the value of the RMB in autumn, which is 1.02, the values are between 1.37 and 2.51, indicating that all of the C6.1 DT3K values match the CALIPSO AOD more closely in the YERB region.

Figure 3 shows the comparative results of MYD04 C6.1 DT10K and CALIPSO AOD. A total of 1211 matches are successfully obtained for CALIPSO AOD_1 and AOD_S. Compared with AOD_1, the matching result of the CALIPSO AOD_S are good, with high *R* values (0.78), nearly 51.78% of the AOD retrievals falling into the EE, and an RMB of 1.2, resulting in only 12% underestimation compared to the MYD04 C6.1 DT10K AOD.

As shown in Table 3, the matching result is a little different for the four seasons, with the R values (AOD_1: 0.69–0.78; AOD_S: 0.72–0.84), the RMSE values (AOD_1: 0.12–0.17; AOD_S: 0.11–0.16), and the within-EE values (AOD_1: 23.38–43.38%; AOD_S: 44.40–60.78%), respectively, and the best matches are observed in spring. On the whole, the C6.1 DT10K AOD tends toward overestimation

Table 2 Comparison of the retrieval accuracy between the CALIPSO AOD for the period of January 1, 2007 to December 31, 2014 and the MYD04 C6.1 DT3K AOD for the period of January 1, 2003 to December 31, 2017 products in the four seasons

Season	CALIPSO AOD	*N*	Slope	*Y*-intercept	R	MAE	RMB	RMSE	Above EE%	Below EE%	Within EE%
Spring	AOD_1	373	0.03	0.18	0.24	0.29	2.51	0.45	4.83	70.78	24.40
	AOD_S	373	0.07	0.24	0.30	0.20	1.74	0.44	5.90	50.94	43.16
Summer	AOD_1	416	0.24	0.13	0.69	0.18	1.81	0.18	6.01	62.98	31.01
	AOD_S	416	0.45	0.13	0.78	0.10	1.32	0.16	8.65	42.79	48.56
Autumn	AOD_1	389	0.32	0.11	0.63	0.07	1.37	0.16	12.85	41.39	45.76
	AOD_S	389	0.53	0.12	0.69	0.00	1.02	0.15	21.08	15.68	63.24
Winter	AOD_1	249	0.03	0.19	0.19	0.20	1.97	0.52	6.83	51.41	41.77
	AOD_S	249	0.05	0.26	0.19	0.12	1.44	0.52	17.67	28.51	53.82

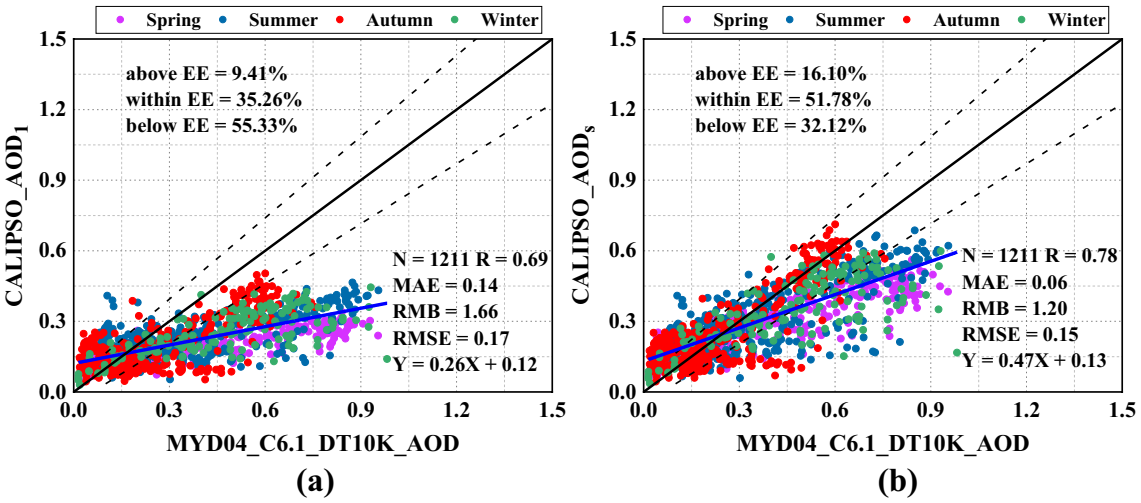

Fig. 3 Validation of the CALIPSO AOD_1 (**a**) and CALIPSO AOD_S (**b**) for the period of January 1, 2007 to December 31, 2014 against MYD04 C6.1 DT10K AOD for the period of January 1, 2003 to December 31, 2017 over the YERB. The black solid line is the 1:1 line, the black dashed lines indicate the envelope of the EE, and the blue line is the regression line

Table 3 Comparison of the retrieval accuracy between the CALIPSO AOD for the period of January 1, 2007 to December 31, 2014 and the MYD04 C6.1 DT10K AOD for the period of January 1, 2003 to December 31, 2017 products in the four seasons

Season	CALIPSO AOD	*N*	Slope	*Y*-intercept	R	MAE	RMB	RMSE	Above EE%	Below EE%	Within EE%
Spring	AOD_1	277	0.17	0.13	0.78	0.23	2.12	0.16	5.05	69.68	25.27
	AOD_S	277	0.36	0.15	0.84	0.13	1.41	0.14	7.22	48.38	44.40
Summer	AOD_1	395	0.25	0.14	0.69	0.14	1.60	0.17	8.61	52.41	38.99
	AOD_S	395	0.48	0.14	0.78	0.05	1.17	0.15	17.72	33.16	49.11
Autumn	AOD_1	385	0.44	0.08	0.76	0.06	1.30	0.12	16.36	40.26	43.38
	AOD_S	385	0.72	0.08	0.82	0.01	0.96	0.11	24.94	14.29	60.78
Winter	AOD_1	154	0.29	0.12	0.72	0.22	1.88	0.16	1.95	74.68	23.38
	AOD_S	154	0.43	0.15	0.72	0.12	1.35	0.16	5.84	44.81	49.35

compared to CALIPSO AOD retrievals for the spring, summer, and winter, except for the AOD_S with MAE = 0.01 and RMB = 0.96 in autumn.

Compared with MYD04 C6.1 DT3K, the MYD04 C6.1 DT10K product has fewer matches in every season but shows large overestimations. This phenomenon is caused mainly by the fact that the MYD04 C6.1 DT3K images had higher resolutions. On the other hand, the reason could be that C6.1 DT10K has few retrievals for the water system over the YERB, as mentioned by (Zhang et al. 2019b).

Figure 4 shows the validation of the MYD04 C6.1 DB10K AOD and CALIPSO AOD over the YERB area. As shown in Fig. 4, a total of 1799 MYD04 C6.1 DB10K-CALIPSO matches are available for AOD_1 and AOD_S. The C6.1 DB10K AOD is well-matched with the CALIPSO AOD_1 and AOD_S, respectively. That is, the *R* values are 0.78 and 0.84 and the percentages within the EE are 34.24 and 53.25%, respectively. A slight overestimation occurs accompanied by MAE values of 0.12 and 0.05, respectively.

Table 4 provides the accuracy statistics for the MYD04 C6.1 DB AOD and CALIPSO AOD products for each season. The accuracy of both products shows apparent seasonal variation in AOD_1 and AOD_S. Comparing the result for all seasons with DT3K and DT10K, there is some degree of improvement in the result of matching of the CALIPSO AOD (AOD_1 and AOD_S) and MYD04 C6.1 DB10K product, with *R* values of 0.77–0.88 for AOD_1 and 0.85–0.90 for AOD_S, respectively, except for DT10K in spring. Comparing the MYD04 C6.1 DB AOD and CALIPSO AOD_1 or AOD_S, the best matches are observed in winter (AOD_1 = 0.88) and autumn (AOD_S = 0.90), with higher *R* values, but the MAE (0.07, 0.12), RMB (1.38, 1.73), and within-EE (50%, 36.97%) values are comparatively better in autumn than in winter for the CALIPSO AOD_1, while the lowest matches are observed in spring. Moreover, unlike the MYD04 C6.1 DT3K and MYD04 C6.1 DT10K products, the MYD04 C6.1 DB10K products show good retrieval accuracy: 450, 450, 450, and 449

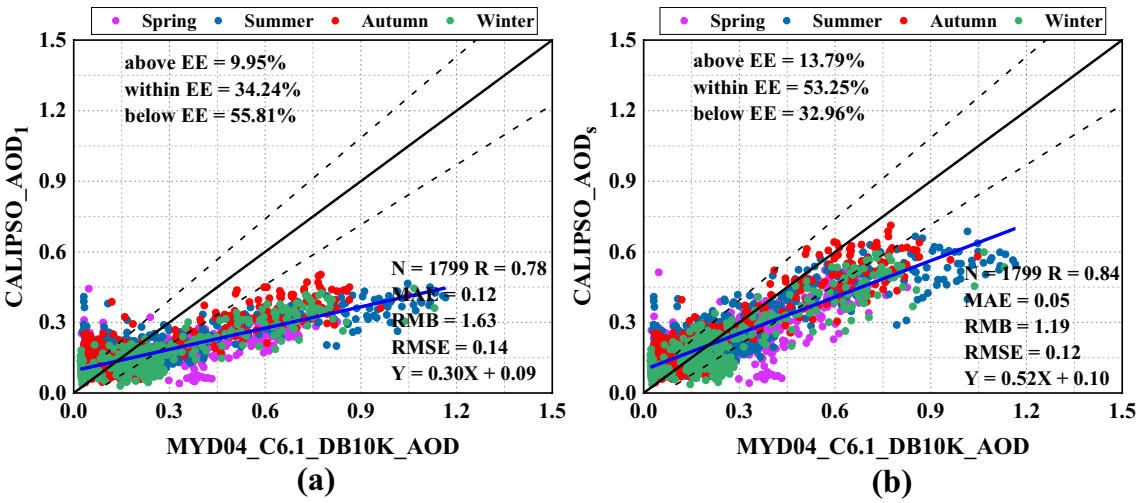

Fig. 4 Validation of the CALIPSO AOD_1 (**a**) and CALIPSO AOD_S (**b**) for the period of January 1, 2007 to December 31, 2014 against MYD04 C6.1 DB10K AOD for the period of January 1, 2003 to December 31, 2017 over the YERB. The black solid line is the 1:1 line, the black dashed lines indicate the envelope of the EE, and the blue line is the regression line

Table 4 Comparison of the retrieval accuracy between the CALIPSO AOD for the period of January 1, 2007 to December 31, 2014 and the MYD04 C6.1 DB10K AOD for the period of January 1, 2003 to December 31, 2017 products in the four seasons

Season	CALIPSO AOD	*N*	Slope	*Y*-intercept	R	MAE	RMB	RMSE	Above EE%	Below EE%	Within EE%
Spring	AOD_1	450	0.21	0.11	0.59	0.16	1.87	0.14	7.11	76.00	16.89
	AOD_S	450	0.47	0.10	0.72	0.08	1.31	0.12	8.89	48.22	42.89
Summer	AOD_1	450	0.23	0.14	0.77	0.13	1.57	0.18	16.00	50.89	33.11
	AOD_S	450	0.43	0.15	0.85	0.05	1.15	0.15	20.89	29.56	49.56
Autumn	AOD_1	450	0.40	0.08	0.86	0.07	1.38	0.12	12.22	37.78	50.00
	AOD_S	450	0.63	0.08	0.90	0.01	1.02	0.10	17.56	16.44	66.00
Winter	AOD_1	449	0.38	0.06	0.88	0.12	1.73	0.10	4.45	58.57	36.97
	AOD_S	449	0.56	0.06	0.89	0.06	1.30	0.10	7.80	37.64	54.57

matches are found for the four seasons, as the DB algorithm can retrieve AOD over complex and bright urban surfaces, whereas the DT algorithm cannot retrieve AOD over such areas. A similar result was also reported by Zhang et al. (2019b).

The evaluation of the MYD04 C6.1 DTB10K AOD and the CALIPSO AOD products over the YERB is presented in Fig. 5. We found 1788 matches of AOD retrievals from MYD04 C6.1 DTB10K and CALIPSO products, with high *R* values (0.76 and 0.83 for CALIPSO AOD_1 and AOD_S products, respectively, and low RMSE values (0.14 and 0.12 for CALIPSO AOD_1 and AOD_S products, respectively. Meanwhile, 51.06% and 59.01% of AOD_1 and AOD_S retrievals, respectively, fell within the EE. At the same time, the RMB values are 1.47 and 1.07, respectively, for AODs and AOD_1, indicating that the C6.1 DTB10K AOD product is overvalued by only 47% and 7% for CALIPSO AOD_S and AOD_1 products, respectively. These results indicate that the value of C6.1 DTB10K AOD is slightly larger than that of CALIPSO, and the degree of matching between AOD_S and C6.1 DTB10K is better.

Table 5 provides the accuracy statistics for the MYD04 C6.1 DTB10K products in each season compared to the CALIPSO AOD products over the YERB region. In the comparison of the MYD04 C6.1 DTB10K product and CALIPSO AOD products, 444, 450, 450, and 444 matches are found for the four seasons. Taking the comparison of AOD_S and MYD04 C6.1 DTB10K as an example, it reveals high accuracies, with within-EE values of 45.05, 53.33, 69.33, and 68.24% for the four seasons (spring, summer, autumn, and winter), along with high *R* values (0.76, 0.90, 0.93, 0.88) and small RMSE values (0.14, 0.11, 0.17, 0.10). The seasonal variation of the maximum within-EE value is 69.33% during autumn and the minimum is 45.05% for spring. Unlike the above products, the overall value of CALIPSO AOD_S is slightly higher than that of MYD04 C6.1 DTB10K product, as shown by a negative MAE (0.01, 0.04), while the RMB (0.96, 0.83) is less than 1 in both summer

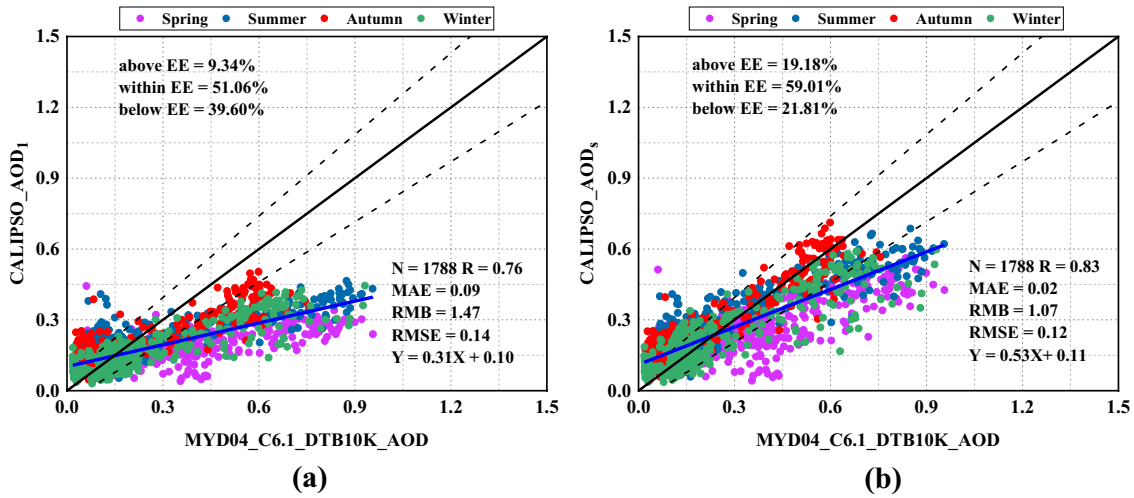

Fig. 5 Validation of the CALIPSO AOD_1 (**a**) and CALIPSO AOD_S (**b**) for the period of January 1, 2007 to December 31, 2014 against MYD04 C6.1 DTB10K AOD for the period of January 1, 2003 to December 31, 2017 over the YERB. The black solid line is the 1:1 line, the black dashed lines indicate the envelope of the EE, and the blue line is the regression line

Table 5 Comparison of the retrieval accuracy between the CALIPSO AOD for the period of January 1, 2007 to December 31, 2014 and the MYD04 C6.1 DTB10K AOD for the period of January 1, 2003 to December 31, 2017 products in the four seasons

Season	CALIPSO AOD	*N*	Slope	*Y*-intercept	R	MAE	RMB	RMSE	Above EE%	Below EE%	Within EE%
Spring	AOD_1	444	0.18	0.12	0.65	0.18	1.98	0.16	4.50	70.05	25.45
	AOD_S	444	0.39	0.12	0.76	0.10	1.38	0.14	7.88	47.07	45.05
Summer	AOD_1	450	0.29	0.14	0.82	0.07	1.31	0.14	14.67	30.44	54.89
	AOD_S	450	0.53	0.15	0.90	0.01	0.96	0.11	30.67	16.00	53.33
Autumn	AOD_1	450	0.51	0.08	0.88	0.02	1.11	0.09	13.11	22.44	64.44
	AOD_S	450	0.80	0.08	0.93	0.04	0.83	0.07	26.67	4.00	69.33
Winter	AOD_1	444	0.39	0.07	0.87	0.08	1.51	0.10	4.95	35.81	59.23
	AOD_S	444	0.58	0.07	0.88	0.03	1.12	0.10	11.26	20.50	68.24

and autumn, respectively. The reason might be that the DTB algorithm not only considers the volume of the target but also includes the dark blue algorithm, which is relatively comprehensive, making for better agreement between the two in their estimates of AOD.

By comparing the matching of products with AOD_1 and AOD_S in different seasons in Tables 2, 3, 4, 5, it is found that the degree of matching between MODIS products and CALIPSO AOD varies to a certain extent, depending on the different MODIS algorithms and resolutions used.

Figures 6 and 7 show box diagrams of the bias between the MYD04 C6.1 AOD retrievals and the CALIPSO AOD retrievals. As shown in Fig. 6, the bias between all MYD04 C6.1 products (with different algorithms or resolutions) and CALIPSO AOD_1 is often greater than 0. According to Fig. 7, although, on the whole, the AOD value of the MYD04 C6.1 product is also larger than the CALIPSO AOD_S, within the range of MODIS AOD < 0.30, most of the CALIPSO AOD_S values are greater than or equal to MYD04 C6.1, indicating that the measured AOD values of the two products are in good agreement there. However, the difference between all MODIS products and CALIPSO AOD_S becomes increasingly negative as MODIS AOD increases for values of MODIS AOD > 0.30. This also indicates that in clean environmental conditions, when atmospheric aerosol levels are low, the difference is small. Algorithmically, the MODIS

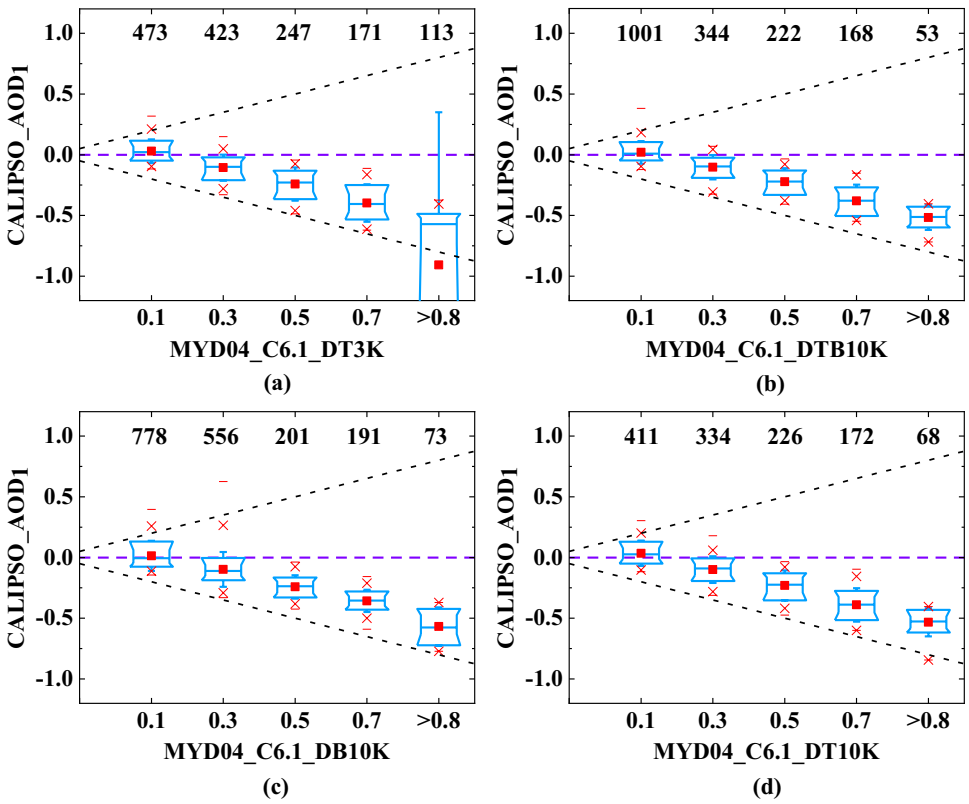

Fig. 6 Box plots of the CALIPSO AOD_1 retrievals for the period of January 1, 2007, to December 31, 2014, against the MYD04 C6.1 AOD retrievals for the period of January 1, 2003, to December 31, 2017, over the YERB. The EE envelopes are within the dashed lines. The number above each box refers to the corresponding matches in the different intervals of the MODIS AOD (0–0.2, 0.2–0.4, 0.4–0.6, 0.6–0.8, and > 0.8). The DT3K, DTB10K, DB10K, and DT10K retrieval biases are presented in (**a**)–(**d**), respectively

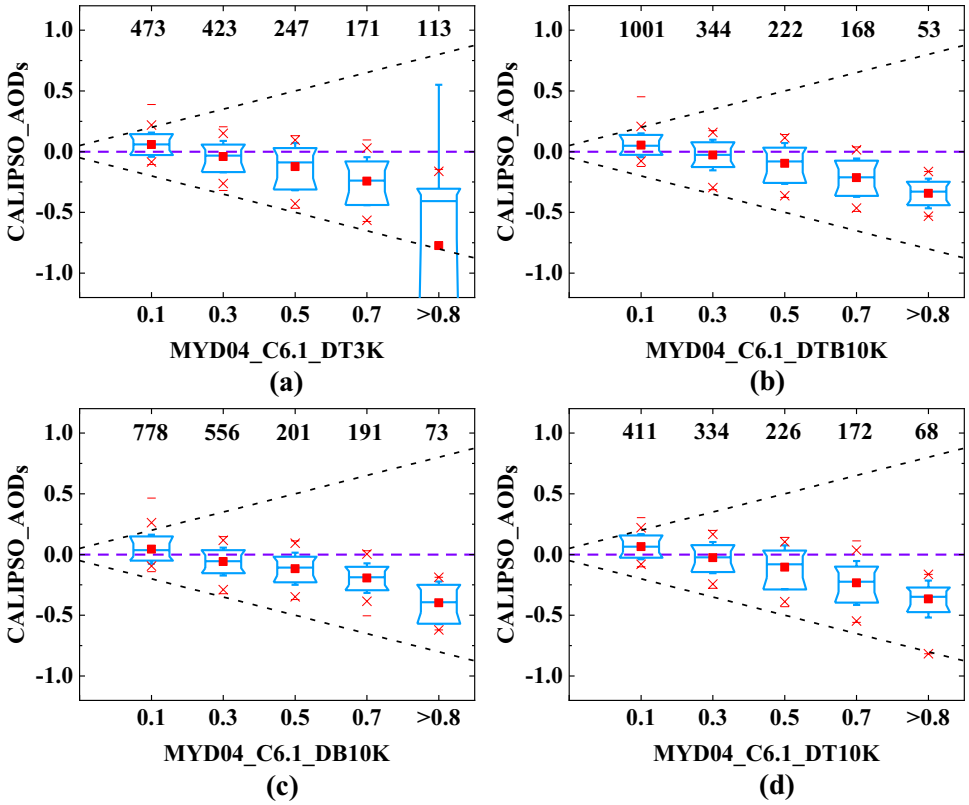

Fig. 7 Box plots of the CALIPSO AOD_S retrievals for the period of January 1, 2007 to December 31, 2014 against the MYD04 C6.1 AOD retrievals for the period of January 1, 2003 to December 31, 2017 over the YERB. The EE envelopes are within the dashed lines. The number above each box refers to the corresponding matches in the different intervals of the MODIS AOD (0–0.2, 0.2–0.4, 0.4–0.6, 0.6–0.8, and > 0.8). The DT3K, DTB10K, DB10K, and DT10K retrieval biases are presented in (**a**)–(**d**), respectively

product considers the radiation extinction of the whole atmosphere (aerosols and gas molecules), while the AOD_S of CALIPSO only considers the extinction of the aerosol layer. Therefore, in clean environmental conditions with low aerosol content, the difference between the two is small. In severe air pollution conditions, the aerosol content is large, both types of AOD are larger, and the difference between the two is also larger.

4.2 Time Series and Regional Variation of AOD Retrieval Bias

Due to large differences in topography, climate, and economic development in the YERB, the region is divided into three sub-regions to study further the comparison between the two products in the time series of these sub-regions.

Figure 8 shows the change curves of MODIS products over the $YERB_1$ region from 2003 to 2017, and CALIPSO products from 2007 to 2014, with different AOD values during each of the four seasons. As can be seen from Fig. 8, the inter-annual variation of the AOD_1 and AOD_S curves in the four seasons are similar, with only a small difference, indicating that the bottom AOD over the $YERB_1$ region undergoes little change over the four seasons, the difference value of AOD in the whole layer remains stable, and the corresponding AOD has a small range of change between different years. This is because the $YERB_1$ region is in the eastern part of the Qinghai–Tibet plateau, where the mountains are cold, the atmosphere is clean, and the overall aerosol content is low. Besides, there is less aerosol stratification there, and the bottom layer of AOD is representative of the full profile of AOD (Zhang et al. 2019b). Also, the value of the bottom layer of AOD over the YERB1 region is relatively high and is close to the value of AOD for the entire atmospheric depth. This might be since the $YERB_1$ region is located in the plateau area, with an average elevation of 3000 m and a high aerosol concentration at low altitude. We found that in summer and fall, there are high and low levels of MODIS products in different years, but in spring and winter, CALIPSO products reported small values throughout the study period. Comparing the four types of MODIS products, for summer and autumn, the difference between them is small, but for spring and especially winter, they exhibit a bigger difference, mainly because the spring and winter DT algorithm products give smaller AOD values, and the obtained data values are all large; at the same time, this also shows that the use of different algorithms in different seasons for the retrieval of AOD leads to a certain difference. Excluding the values of DT3K and DT10K in winter, the overall AOD values were higher in spring and summer than in autumn and winter. Another reason might be that in spring and winter in the mountain plateau areas, the temperature difference is large, which has

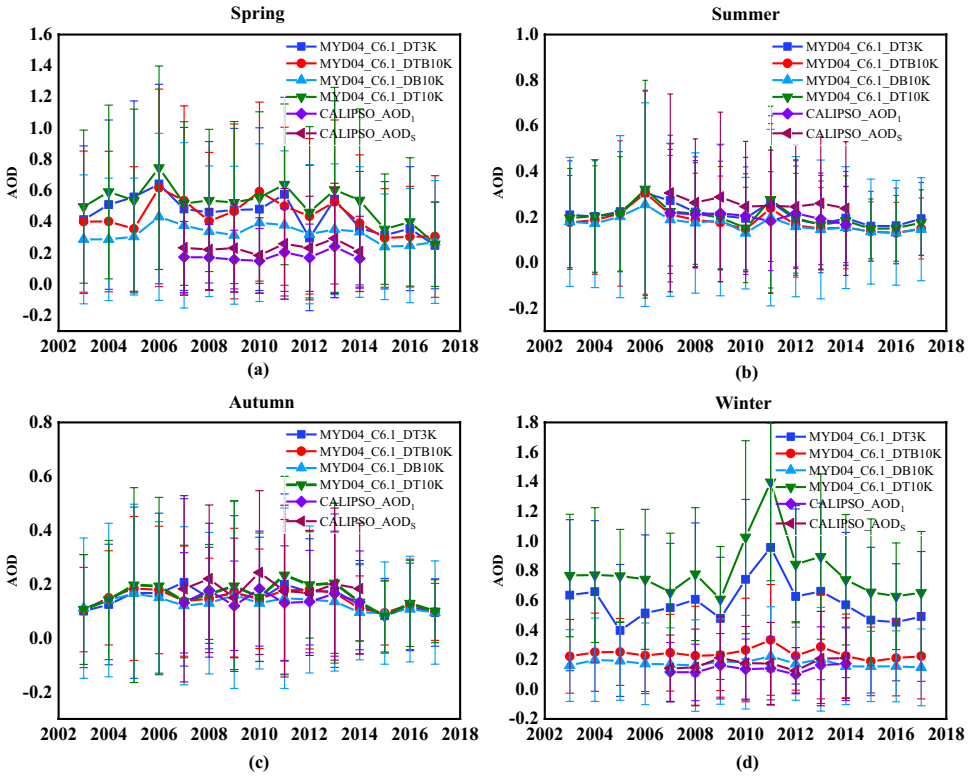

Fig. 8 Time series of AOD changes for the MYD04 C6.1 product from January 2003 to December 2017 and CALIPSO AOD product from January 2007 to December 2014 in the four seasons over the $YERB_1$ region

a certain influence on the change of atmospheric aerosol content, resulting in a large difference in spring and winter products.

Figure 9 shows the change curves of MODIS products over the $YERB_2$ region from 2003 to 2017, and CALIPSO products from 2007 to 2014, with different AOD values during each of the four seasons. As can be seen from Fig. 9, the change between the four seasons in the same region generally follows the order: summer > spring > winter > autumn. Among them, the inter-annual variation of the AOD_1 and AOD_S curves for the four seasons are similar, and the changes in different values are relatively small, but the difference value of AOD_1 and AOD_S in each year is greater than that of the $YERB_1$ region. This might be because the $YERB_2$ region is predominantly loess plateau. Compared with the $YERB_1$ region, the altitude is lower and the vertical stratification of the atmosphere is stronger. As a result, the aerosol stratification intensity is relatively high, and consequently, the AOD of the bottom layer is less than that of the full profile (Zhang et al. 2019b).

Comparing the curves of the two products, it is found that the AOD_S values in summer, autumn, and winter are slightly greater than those of DTB10K AOD in almost all years (this might be caused by DTB's combination of the dark target and dark blue algorithms). Other DT10K, DB10K, and DT3K products in different years have high and low values, but for the spring, in almost all years, the AOD values given by the four MODIS products are greater than those obtained by CALIPSO. This might be because a large number of sandstorms occur in the loess plateau area in spring, and thus a large number of dust aerosols will appear. As stated earlier, this increase in dust aerosol content will cause the AOD by MODIS to be greater than that of CALIPSO. By comparing the four MODIS products, it is found that the AOD values of DTB are the smallest in almost every year, in each of the four seasons over the $YERB_2$ region, while DT10K AOD is maximal and DT3K AOD is medium in different seasons, respectively. This pattern is completely different from that of the $YERB_1$ region, indicating that the inversion of AOD by MODIS products over different regions is quite different, as is also reflected in our previous research results (Zhang et al. 2019a; b).

Figure 10 shows the change curves of MODIS products over the $YERB_3$ region, from 2003 to 2017, and CALIPSO products, from 2007 to 2014, with different AOD values during each of the four seasons. As can be seen from Fig. 10, the inter-annual variation curves of AOD_1 and AOD_S are similar for the four seasons, but the differences between AOD_1 and AOD_S are larger than over the $YERB_1$ and YERB2 regions, indicating that the difference value between AOD_1 and AOD_S increases with the decrease in altitude, for the reasons explained above. MODIS AOD is greater than CALIPSO AOD in the four seasons in almost all years, but the difference between the four MODIS products varied significantly among the four seasons. Among them, the difference between DT3K and DT10K products in the four

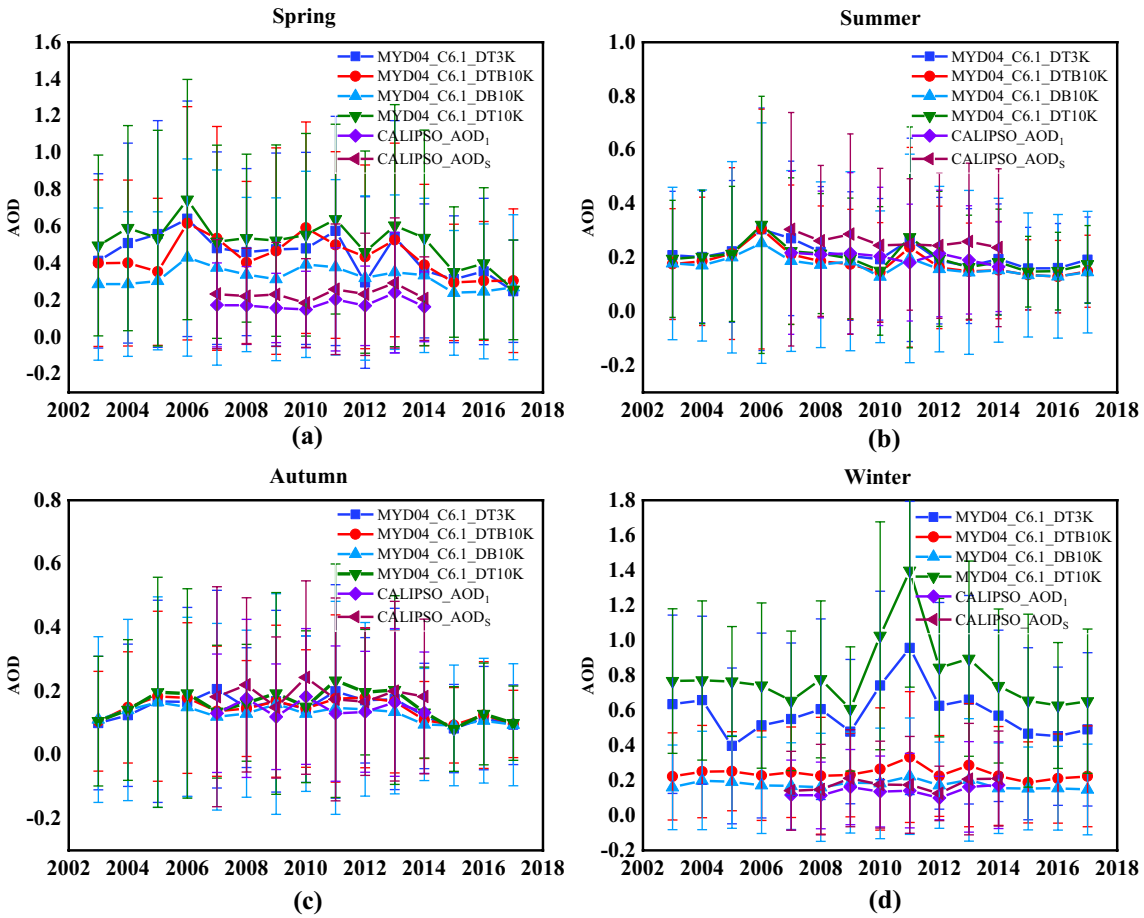

Fig. 9 Time series of AOD changes for the MYD04 C6.1 product from January 2003 to December 2017 and CALIPSO AOD product from January 2007 to December 2014 in the four seasons over the $YERB_2$ region

seasons is smaller, except that the DB10K AOD value in spring is found to the smallest in each year, while the other three seasons exhibit the highest values and show a different pattern than over the $YERB_1$ and $YERB_2$ regions, indicating that the aerosol load of DB and DT algorithm products has a large correlation over the region. A comprehensive picture can be observed from Figs. 8, 9, and 10; on the whole, the degree of matching of the MODIS and CALIPSO products follow the order: $YERB_1 > YERB_2 > YERB_3$, indicating that under the lower aerosol load, the AOD retrieval values of the two products are closer.

By comparing the AOD values of different regions for the same season in Figs. 8, 9, and 10, it is found that, in spring and winter, the overall average value of MODIS products generally follows the order: $YERB_3 > YERB_1 > YERB_2$. In summer and autumn, MODIS products generally follow the order $YERB_3 > YERB_2 > YERB_1$, indicating that the value of AOD acquired by MODIS products is influenced by both seasonal and regional factors. In all four seasons, CALIPSO products follow the order: $YERB_3 > YERB_2 > YERB_1$. This pattern occurs because the $YERB_3$ region is located in the north China plain, which has a high aerosol load (Che et al. 2013; Chen et al. 2017; He et al. 2018; Tao et al. 2017). Overall, the results (Figs. 2, 3, 4, 5, 6, 7, 8, 9, 10 and Tables 2, 3, 4, 5) show that there are degrees of variation for several MODIS C6.1 products. Previously, we reported the comparison between MODIS products and the ground-based CARSNET data and found that currently no MODIS aerosol product is suitable for the whole YERB region and that it is a challenging task to obtain high-quality AOD retrievals for such large areas. In this paper, the results of CALIPSO also show a big difference over each region. On the whole, it can be concluded that the retrieval and measurement values of AOD of several products have an excellent relationship with the different seasons, sub-regions, and terrains.

4.3 Spatial Distribution of MYD04 C6.1 and CALIPSO AOD

To the best of our knowledge, the optical and physical properties of aerosol in the YERB given by MODIS products have not yet been studied. Figure 11 shows that the AOD

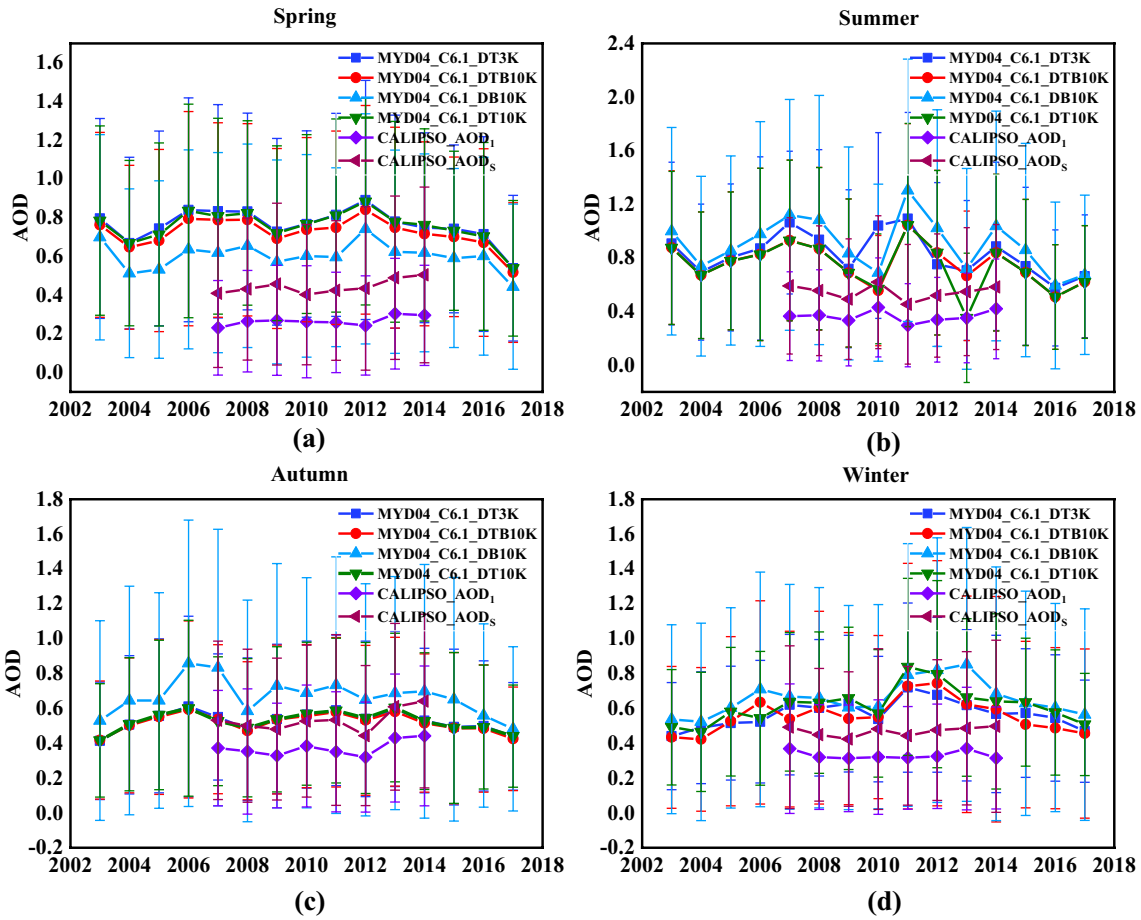

Fig. 10 Time series of AOD changes for the MYD04 C6.1 product from January 2003 to December 2017 and CALIPSO AOD product from January 2007 to December 2014 in the four seasons over the $YERB_3$ region

values of the three sub-regions have obvious regional characteristics; AOD values over the $YERB_3$ sub-region are significantly higher than those over the other two areas. This pattern might be due to the fact that relative to the $YERB_1$ and $YERB_2$ regions, the $YERB_3$ region has a relatively well-developed economy, and so industrial and vehicle aerosol emissions are higher there. First, AOD_1 is the AOD of the lowest aerosol layer, so AOD_1 is all lower than other products. Second, the eastern part of YERB (YERB3) is the plain area, the economy is developed, anthropogenic emissions are high, especially in winter. The summer and autumn also are the harvest season, crops Straw burning activities were also frequent and leading to high aerosol emissions and high AOD.

Several products generally show that the AOD values in spring and summer are greater than that in autumn and winter, which might be due to the straw burning in the $YERB_3$ region, which might, in turn, lead to an increase in anthropogenic aerosol content in spring and summer. High AOD values over the $YERB_1$ and $YERB_2$ sub-regions might be due to the increase of natural aerosol content caused by wind-blown sand in spring and summer, and due to the increase of dust emitted from the loess plateau.

Furthermore, MYD04 C6.1 DT3K and DT10K aerosol products have not retrieved the corresponding AOD values in some areas in the north and east of the basin, especially in winter. This large area has no data, which might due to the low single scattering reflectance over the snow surface. Because the Qinghai–Tibet plateau and part of the loess plateau are often covered by snow in winter.

5 Conclusions

In this paper, CALIPSO AOD products from 1 January 2007 to 31 December 2014 are evaluated in comparison with MODIS MYDO4 C6.1 AOD products from 1 January 2003 to 31 December 2017 over the YERB. This study concludes that: The distribution of AOD values obtained from CALIPSO and MODIS are significantly different over three different regions of YERB, and this difference is closely related to the season, sub-region, and

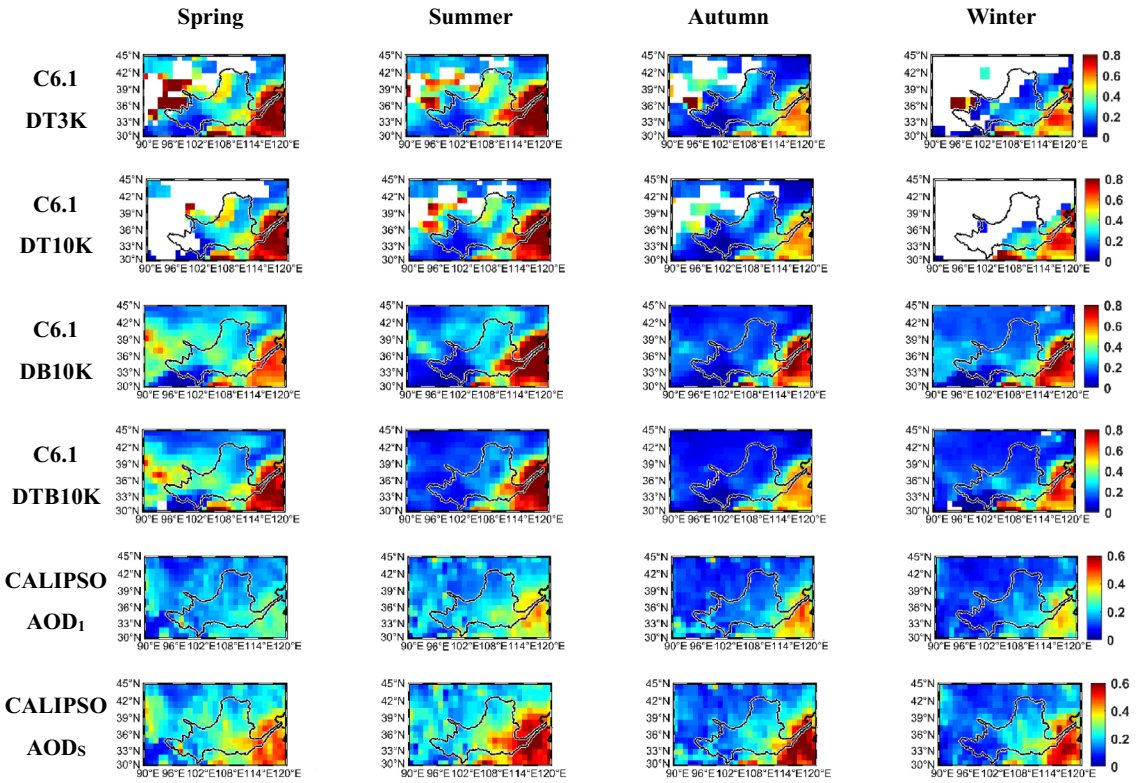

Fig. 11 Spatial distribution of the MYD04 C6.1 AOD for the period of January 1, 2003 to December 31, 2017 and the CALIPSO AOD_1 retrievals for the period of January 1, 2007 to December 31, 2014 in the four seasons over the YERB. The color scale refers to the AOD values

topography. As a whole, the CALIPSO products' AOD retrievals underestimate the MODIS AOD products, while no single satellite AOD product is suitable for the whole of the YERB region. The degree of matching between the CALIPSO AOD_S and the MODIS product is significantly higher than that of AOD_1; the MODIS and the CALIPSO AOD_S products are well matched within the range of MODIS AOD < 0.30, while the degree of matching decreases as MODIS AOD increases within the range of MODIS AOD > 0.30. All the products we investigated here generally reveal the pattern that the AOD retrievals of spring and summer are larger than those of autumn and winter and the difference in AOD retrievals by all these products is the smallest in autumn. In spring and winter, the overall average value of MODIS products generally follows the order: $YERB_3 > YERB_1 > YERB_2$, while in summer and autumn, MODIS products generally follow the order: $YERB_3 > YERB_2 > YERB_1$. For all four seasons, CALIPSO products follow the order: $YERB_3 > YERB_2 > YERB_1$. This is closely related to the topographic factors of the YERB. Based on the season, sub-region, and other factors, the CALIPSO AOD retrievals have the best consistency with the MYD04 C6.1 DTB10K product, while they have the lowest consistency with MYD04 C6.1 DT3K. The performance of DTB10K is better than DT3K although it has the coarser spatial resolution, it has the best consistency with CALIPSO. CALIPSO AOD products can be used for AOD retrieval analysis for such large and diverse topographic areas.

Acknowledgements We thank NASA for providing datasets of Aqua-MODIS and CALIPSO. We would also like to thank the editors for modifying and revising this manuscript.

Author contributions Conceptualization: ZZ and MZ; Software: BS, CZ; Validation: ZZ, MB, and LG; Investigation: ZZ and MZ; Writing—original draft: ZZ; Curation: MZ and ZZ; All authors read the manuscript, contributed to the discussion, and agreed to the published version of the manuscript.

Funding This work was supported by the National Natural Science Foundation of China (Grant Number 41801282), Programs for Science and Technology Development of Henan Province (Grant Numbers 202102310294, 192102310008), the Nanyang Normal University Scientific Research Project (Grant Number ZX2018020), and the National College Students Innovation and Entrepreneurship training Program (No.202010481053, 202010481049).

Compliance with Ethical Standards

Conflict of interest The authors declare no conflict of interest.

References

Ali MA, Assiri M (2019) Analysis of AOD from MODIS-merged DT–DB products over the Arabian Peninsula. Earth Syst Environ 3(3):625–636

Ali MA, Islam MM, Islam MN, Almazroui M (2019) Investigations of MODIS AOD and cloud properties with CERES sensor based net cloud radiative effect and a NOAA HYSPLIT Model over Bangladesh for the period 2001–2016. Atmos Res 215:268–283

Ali MA et al (2020) Classification of aerosols over Saudi Arabia from 2004–2016. Atmos Environ 241:117785

Bilal M, Nichol JE, Bleiweiss MP, Dubois D, Rse J (2013) A Simplified high resolution MODIS aerosol retrieval algorithm (SARA) for use over mixed surfaces. Remote Sens Environ 136:135–145

Bilal M, Nichol JE, Chan PW (2014) Validation and accuracy assessment of a simplified aerosol retrieval algorithm (SARA) over Beijing under low and high aerosol loadings and dust storms. Remote Sens Environ 153:50–60

Bilal M, Qiu Z, Campbell JR, Scott S, Shen J, Nazeer M (2018) A New MODIS C6 dark target and deep blue merged aerosol product on a 3 km spatial grid. Remote Sens 10:463

Bilal M et al (2019) Evaluation of Terra-MODIS C6 and C6.1 aerosol products against Beijing, XiangHe, and Xinglong AERONET Sites in China during 2004–2014. Remote Sens 11:486

Butt EW et al (2016) The impact of residential combustion emissions on atmospheric aerosol, human health, and climate. Atmos Chem Phys 16:873–905

Che H et al (2013) Column aerosol optical properties and aerosol radiative forcing during a serious haze-fog month over North China Plain in 2013 based on ground-based sunphotometer measurements. Atmos Chem Phys 14:2125–2138

Che H et al (2014) Column aerosol optical properties and aerosol radiative forcing during a serious haze-fog month over North China plain in 2013 based on ground-based sunphotometer measurements. Atmos Chem Phys 14:2125–2138

Che H et al (2015) Ground-based aerosol climatology of China: aerosol optical depths from the China aerosol remote sensing network (CARSNET) 2002–2013. Atmos Chem Phys 15:7619–7652

Chen W, Fan A, Yan L (2017) Performance of MODIS C6 aerosol product during frequent haze-fog events: a case study of Beijing. Remote Sens 9:496

Deng X et al (2008) Effects of Southeast Asia biomass burning on aerosols and ozone concentrations over the Pearl River Delta (PRD) region. Atmos Environ 42:8493–8501

Development IPoCCWGIIJE (2014) Climate change 2014: mitigation of climate change. Chapter 8: transport: final draft

Dubovik O, Smirnov A, Holben BN, King MD, Kaufman YJ, Eck TF, Slutsker I (2012) Accuracy assessments of aerosol optical properties retrieved from aerosol robotic network (AERONET) Sun and sky radiance measurements. J Geophys Res Atmos 105:9791–9806

Edenhofer O, Seyboth K (2013) Intergovernmental panel on climate change (IPCC)

Gong W, Zhang M, Han G, Ma X, Zhu Z (2015) An investigation of aerosol scattering and absorption properties in Wuhan, Central China. Atmosphere 6:503–520

Gupta P, Levy RC, Mattoo S, Remer LA, Munchak LA (2016) A surface reflectance scheme for retrieving aerosol optical depth over urban surfaces in MODIS dark target retrieval algorithm. Atmos Meas Tech 9:3293–3308

Han G, Xu H, Wei G, Liu J, Du J, Ma X, Liang A (2018) Feasibility study on measuring atmospheric CO_2 in urban areas using spaceborne CO_2-IPDA LIDAR. Remote Sens 10:985

He L, Wang L, Lin A, Ming Z, Bilal M, Tao M (2017) Aerosol optical properties and associated direct radiative forcing over the Yangtze River Basin during 2001–2015. Remote Sens 9:746

He L, Wang L, Lin A, Zhang M, Bilal M, Wei J (2018) Performance of the NPP-VIIRS and aqua-MODIS aerosol optical depth products over the Yangtze River Basin. Remote Sens 10:117

Hsu NC et al (2013) Enhanced deep blue aerosol retrieval algorithm: the second generation. J Geophys Res 118:9296–9315

Huang J et al (2008) An overview of the semi-arid climate and environment research observatory over the Loess plateau. Adv Atmos Sci 25:906–921

Jie Z et al (2017) Validation of MODIS C6 AOD products retrieved by the dark target method in the Beijing–Tianjin–Hebei urban agglomeration, China. Adv Atmos Sci 34:993–1002

Jing W, Lin S, Bo H, Bilal M, Wang L (2018) Verification, improvement and application of aerosol optical depths in China. Part 1: inter-comparison of NPP-VIIRS and Aqua-MODIS. Atmos Environ 175:221–233

Kaiser J, Granmar M (2005) Epidemiology. Mounting evidence indicts fine-particle pollution. Science 307:1858–1861. https://doi.org/10.1126/science.307.5717.1858a

Kang N, Kumar KR, Hu K, Yu X, Yin Y (2016) Long-term (2002–2014) evolution and trend in collection 5.1 level-2 aerosol products derived from the MODIS and MISR sensors over the Chinese Yangtze River Delta. Atmos Res 181:29–43

Kato S, Loeb NG, Rutan DA, Rose FG, Sun-Mack S, Miller WF, Yan C (2012) Uncertainty estimate of surface irradiances computed with MODIS-, CALIPSO-, and CloudSat-Derived cloud and aerosol properties. Surv Geophys 33:395–412

Kaufman YJ, Tanre D, Boucher O (2002) A satellite view of aerosols in the climate system. Nature 419:215–223. https://doi.org/10.1038/nature01091

Kleidman RG et al (2005) Comparison of moderate resolution imaging spectroradiometer (MODIS) and aerosol robotic network (AERONET) remote-sensing retrievals of aerosol fine mode fraction over ocean. J Geophys Res 110:D22205

Kulmala M et al (2013) Direct observations of atmospheric aerosol nucleation. Science 339:943–946. https://doi.org/10.1126/science.1227385

Kumar A, Singh N, Solanki R (2018) Evaluation and utilization of MODIS and CALIPSO aerosol retrievals over a complex terrain in Himalaya. Remote Sens Environ 206:139–215

Lelieveld J, Evans JS, Fnais M, Giannadaki D, Pozzer A (2015) The contribution of outdoor air pollution sources to premature mortality on a global scale. Nature 525:367–371

Levy RC, Mattoo S, Munchak LA, Remer LA, Sayer AM, Patadia F, Hsu NC (2013) The collection 6 MODIS aerosol products over land and ocean. Atmos Meas Tech 6:2989–3034

Liu Z et al (2008) Airborne dust distributions over the Tibetan Plateau and surrounding areas derived from the first year of CALIPSO lidar observations. Atmos Chem Phys 8:5045–5060

Magistrale V (1992) Health aspects of air pollution. Springer, Berlin

Marchant B, Platnick S, Meyer K, Wind G (2020) Evaluation of the Aqua MODIS Collection 6.1 multilayer cloud detection algorithm through comparisons with CloudSat CPR and CALIPSO CALIOP products. Atmos Meas Tech 13:3263–3275

Miao Z, Liu J, Bilal M, Zhang C, Nazeer M, Atique L, Han G, Gong W (2020) Aerosol optical properties and contribution to differentiate haze and haze-free weather in Wuhan City. Atmophere 11:322

Ming Z, Wang L, Wei G, Ma Y, Liu B (2017) Aerosol optical properties and direct radiative effects over Central China. Remote Sens 9:997

Misra A, Jayaraman A, Ganguly D (2008) Validation of MODIS derived aerosol optical depth over Western India. J Geophys Res Atmos 113:D04203

Nichol JE, Bilal M, Ali MA, Qiu Z (2020) Air pollution scenario over China during COVID-19. Remote Sens 12:2100

Omar AH, Winker DM, Vaughan MA, Hu Y, Trepte CR, Ferrare RA et al (2009) The Calipso automated aerosol classification and lidar ratio selection algorithm. J Atmos Ocean Technol 26:1994–2014

Qin W et al (2018) Characteristic and driving factors of aerosol optical depth over Mainland China during 1980–2017. Remote Sensing 10:1064

Rosenfeld D (2000) Suppression of rain and snow by urban and industrial air pollution. Science 287:1793–1796. https://doi.org/10.1126/science.287.5459.1793

Shen XJ et al (2015) Characterization of submicron aerosols and effect on visibility during a severe haze-fog episode in Yangtze River Delta, China. Atmos Environ 120:307–316

Shi H, Xiao Z, Zhan X, Ma H, Tian X (2019) Evaluation of MODIS and two reanalysis aerosol optical depth products over AERONET sites. Atmos Res 220:75–80

Shi Y, Liu B, Chen S, Gong W, Jin Y (2020) Characteristics of aerosol within the nocturnal residual layer and its effects on surface PM2.5 over China. Atmos Environ 241:117841

Sun J, Ariya PA (2006) Atmospheric organic and bio-aerosols as cloud condensation nuclei (CCN): a review. Atmos Environ 40:795–820

Tao M et al (2017) How do aerosol properties affect the temporal variation of MODIS AOD bias in Eastern China. Remote Sens 9:800

Tian X, Liu Q, Li X, Wei J (2018) Validation and comparison of MODIS C6.1 and C6 aerosol products over Beijing. China. Remote Sens 10:2021

Tie X, Wu D, Brasseur G (2009) Lung cancer mortality and exposure to atmospheric aerosol particles in Guangzhou, China. Atmos Environ 43:2375–2377

Wang H, Yang Z, Saito Y, Liu JP, Wang Y (2007) Stepwise decreases of the Huanghe (Yellow River) sediment load (1950–2005): impacts of climate change and human activities. Glob Planet Change 57:331–354

Wang Y, Yuan Q, Li T, Shen H, Zheng L, Zhang L (2019) Evaluation and comparison of MODIS Collection 6.1 aerosol optical depth against AERONET over regions in China with multifarious underlying surfaces. Atmos Environ 200:280–301

Winker DM, Pelon J, Mccormick MP (2003) The CALIPSO mission: spaceborne lidar for observation of aerosols and clouds. Proc Spie 4893:1211–1229

Winker DM, Hunt WH, Mcgill M (2007) Initial performance assessment of CALIOP. Geophys Res Lett 34:228–262

Winker DM et al (2009) Overview of the CALIPSO mission and CALIOP data processing algorithms. J Atmos Ocean Technol 26:2310–2323

Xia X et al (2016) Ground-based remote sensing of aerosol climatology in China: aerosol optical properties, direct radiative effect and its parameterization. Atmos Environ 124:243–251

Yang Y, Wu J, Bai L, Wang B (2020) Reliability of gridded precipitation products in the Yellow River Basin, China. Remote Sens 12:374

Yu H, Chin M, Yuan T, Bian H, Zhao C (2015) The fertilizing role of african dust in the amazon rainforest: a first multiyear assessment based on CALIPSO Lidar observations. Geophys Res Lett 42:1984–1991

Zhang MM, Liu ZB, Yun-Jian GE, Basin EY (2014a) Spatio-temporal distribution of atmospheric aerosol optical depth in Jiangsu Province

Zhang M, Gong W, Zhu Z (2014b) Aerosol optical properties of a haze episode in Wuhan based on ground-based and satellite observations. Atmosphere 5:699–719

Zhang M, Liu J, Bilal M, Zhang C, Zhao F, Xie X, Khedher KM (2019a) Optical and physical characteristics of the lowest aerosol layers over the Yellow River Basin. Atmosphere 10:638

Zhang M et al (2019b) Evaluation of the aqua-MODIS C6 and C6.1 aerosol optical depth products in the Yellow River Basin, China. Atmosphere 10:426